https://doi.org/10.3799/dqkx.2026.071

热液金成矿系统流体运移通道三维重建及找矿预测

刘占坤[1,2],郝子和[1,2],邓 浩[1,2*],陈煜东[1,2,3],吴路波[4],
黄珏璇[1,2],陈 进[1,2],毛先成[1,2]

1. 有色金属成矿预测与地质环境监测教育部重点实验室,中南大学地球科学与信息物理学院,湖南长沙 410083
2. 有色资源与地质灾害探查湖南省重点实验室,湖南长沙 410083
3. 中国科学技术大学地球和空间科学学院,安徽合肥 230026
4. 招金矿业股份有限公司,山东烟台 265400

摘 要: 热液成矿流体运移通道控制了热液流体的空间运移与汇聚成矿,三维重建流体通道对理解矿床成因、开展找矿预测至关重要.然而现有研究受限于采样成本高昂、研究方法定性和地质特征复杂,难以在矿床尺度重建成矿流体运移通道三维结构.本研究以胶东夏甸金矿床为研究对象,设计了一种知识-数据协同驱动的流体通道三维重建方法框架.该框架基于矿床地质调查、勘查数据(例如钻孔、中段编录数据)确定流体通道识别标志,通过图卷积深度网络模型构建流体通道空间概率分布模型,基于马尔科夫链模型定量表征三维成矿流体运移通道.实验结果表明:(1)该模型在小样本数据条件下表现出优异的特征识别能力(AUC=0.956 9),推断的流体运移通道高概率区域与成矿流体流动认识相符;(2)夏甸金矿成矿流体来源于深部,沿招平断裂带向上呈分支扩散状运移;(3)主干流体通道分布主要受招平断裂深部产状变化控制,而密集发育的次级通道网络受次级断裂、节理、裂隙等构造控制,反映了流体运移、矿质沉淀的协同控矿作用.本研究为理解构造-流体-矿化耦合机制提供了新视角,揭示了夏甸金矿"主干通道运移-分支末端沉淀"的流体流动模式,基于流体运移通道特征圈定了夏甸金矿深部2处成矿有利区.

关键词: 成矿流体运移通道;三维地质建模;图卷积网络;马尔科夫链模型;夏甸金矿;机器学习;矿床学.
中图分类号: P628 **文章编号:** 1000-2383(2026)03-881-15 **收稿日期:** 2025-12-30

3D Reconstruction of Fluid Migration Pathways of Hydrothermal Gold Systems and Prospecting Prediction

Liu Zhankun[1,2], Hao Zihe[1,2], Deng Hao[1,2*], Chen Yudong[1,2,3], Wu Lubo[4],
Huang Juexuan[1,2], Chen Jin[1,2], Mao Xiancheng[1,2]

1. *Key Laboratory of Metallogenic Prediction of Nonferrous Metals and Geological Environment Monitoring (Ministry of Education), School of Geosciences and Info-Physics, Central South University, Changsha* 410083, *China*
2. *Hunan Key Laboratory of Nonferrous Resources and Geological Hazard Detection, Changsha* 410083, *China*
3. *School of Earth and Space Sciences, University of Science and Technology of China, Hefei* 230026, *China*
4. *Zhaojin Mining Industry Co., Ltd., Yantai* 265400, *China*

基金项目: 国家自然科学基金项目(Nos. 42202332, 42472362, 42272344, 41972309).
作者简介: 刘占坤(1992—),男,博士,副教授,主要从事成矿系统定量解析与三维预测研究. ORCID:0000-0002-3734-1138. E-mail: zkliu0322@csu.edu.cn
* **通讯作者:** 邓浩, ORCID:0000-0001-9417-6629. E-mail:haodeng@csu.edu.cn

引用格式: 刘占坤,郝子和,邓浩,陈煜东,吴路波,黄珏璇,陈进,毛先成,2026.热液金成矿系统流体运移通道三维重建及找矿预测.地球科学,51(3):881-895.
Citation: Liu Zhankun, Hao Zihe, Deng Hao, Chen Yudong, Wu Lubo, Huang Juexuan, Chen Jin, Mao Xiancheng, 2026.3D Reconstruction of Fluid Migration Pathways ofHydrothermal Gold Systems and Prospecting Prediction.*Earth Science*,51(3):881-895.

Abstract: Three-dimensional reconstruction of fluid pathways is critical to understanding ore genesis and guiding exploration since hydrothermal fluid migration pathways exert a fundamental control on the transport, concentration, and precipitation of ore-forming fluids. However, robust three-dimensional reconstruction of fluid pathways at the deposit scale remains challenging due to complex structural overprinting, sparse sampling, and limited quantitative tools. Here, we present an integrated knowledge and data-driven framework to reconstruct the 3D hydrothermal fluid migration pathways of the Xiadian gold deposit in the Jiaodong Peninsula. Geological indicators related to fluid flow were extracted from drill-hole and mine-level datasets and incorporated into a spatial probability model using a Graph Convolutional Network (GCN). A Markov chain model was subsequently applied to quantitatively trace three-dimensional migration trajectories. The GCN demonstrates strong predictive performance under small-sample conditions (AUC=0.956 9), delineating high-probability fluid pathways that are consistent with established metallogenic models. The reconstructed pathways indicate that ore-forming fluids originated at depth and migrated upward along the Zhaoping Fault Zone, exhibiting a branching and diffusive architecture. Major fluid conduits are primarily controlled by deep-seated structural variations of the main fault, whereas dense terminal branch networks are dominated by secondary faults and fracture systems, reflecting a synergistic structural control on fluid migration and mineral precipitation. The results confirm the existence of a conceptual model of "transport along major conduits and precipitation within terminal branches" in Xiadian gold deposit, providing new insights into the coupling between tectonics, fluid flow, and mineralization. On this basis, two prospective targets for deep exploration within the Xiadian deposit are identified.

Key words: ore-forming fluid migration pathway; 3D geological modeling; graph convolutional networks; Markov chain model; Xiadian gold deposit; machine learning; ore deposits.

0 引言

热液型金矿床的形成过程涉及成矿流体从源区向成矿部位的输运、富集以及与围岩、构造发生的复杂物理化学反应(Sibson *et al.*, 1988;翟裕生, 1999; Yang *et al.*, 2012; Henry *et al.*, 2014; Chai *et al.*, 2017; Yang *et al.*, 2018). 在热液金成矿系统中,流体通道是连接成矿流体源区、转移运输与矿化定位的核心纽带,其不仅是流体与矿质迁移的物理通道,也常是矿质沉淀的重要场所,其形成、演化与结构特征直接决定了金矿的形成、定位与规模(邓军等, 2005; Koegelenberg *et al.*, 2016; Deng *et al.*, 2024; Xiao *et al.*, 2024;杨立强等, 2024). 因此,查明成矿流体运移通道的空间位置、揭示其三维结构,对于查明成矿机理和发现深边部矿产资源具有重要意义.

现有成矿流体运移通道研究一般从矿化-蚀变分带(郭涛等, 2008)、成矿构造(Cowan, 2020; Liu *et al.*, 2021a)、流体包裹体(Deng *et al.*, 2003; Launay *et al.*, 2018)、元素/同位素(Hickey *et al.*, 2014; Torremans *et al.*, 2018; Hood *et al.*, 2019)等方面入手,寻找流体运移通道标志,综合推断古成矿流体通道的可能位置.但这些研究主要基于传统的地质、化验等数据对流体通道进行分析推断,其虽然能够对流体的运移通道进行定位,但对运移通道的空间结构尚缺乏认识,难以实现三维重建.近年来,面向矿床尺度的勘查数据挖掘与机器学习研究快速发展(左仁广, 2021,周永章和肖凡, 2024;成秋明, 2025;毛先成等, 2026;左仁广等, 2026),主要体现在:(1)基于多源勘查数据的矿床三维结构化建模技术更为先进,使断裂、蚀变带、矿体等关键地质对象能够被高质量地定量表征与分析(侯卫生等, 2007;郭甲腾等, 2019; Chen *et al.*, 2020, 2024a;毛先成等, 2024);(2)基于机器学习/深度学习的数据挖掘、智能预测研究进展明显,有力地支撑了潜在规律的发现和地质体空间分布位置推断(Xiang *et al.*, 2020; Xiong and Zuo, 2020; Zuo, 2020;左仁广等, 2021; Zuo and Xu, 2023;王智宇等, 2025);(3)面向成矿过程要素(构造-流体-能量耦合)的定量表征与数值模拟,能较好地分析岩浆流动或构造变形驱动下的热液流体运移特征与规律(Li *et al.*, 2017;安文通等, 2021;韩润生等, 2025; Mao *et al.*, 2024a).因此,若能从勘查数据中分析矿体、蚀变带、构造等与成矿流体流动密切相关的地质对象,并通过机器学习等数据挖掘技术分析流体通道位置,则有可能系统地获取流体通道空间结构信息,进而实现流体运移通道三维重建.

综上,本文提出一种知识-数据协同驱动的流体通道三维重建方法框架.通过地质调查、勘查编录信息确定流体通道标志,进而在三维空间中通过深度学习挖掘流体通道空间位置信息.考虑到流体通道这类地质对象具有复杂的拓扑结构,传统的规

则网格化深度学习方法可能难以有效表征相关信息,本文选择图卷积网络(Graph Convolutional Networks, GCN)(Kipf and Welling,2017)来推断成矿空间中流体通道相关体元之间的空间邻接与拓扑关系.在流体通道空间位置信息推断的基础上,笔者拟选择时空连续的马尔科夫(Markov)过程(Rubin,2003)模拟并重建符合流体时空运移的成矿流体三维运移轨迹,实现三维成矿流体运移通道的定位和可视化.本文将上述方法应用在胶东半岛夏甸金矿床,开展热液金矿床流体运移通道三维重建,并进一步开展找矿预测.

1　夏甸金矿地质背景

胶东半岛是我国最大的金成矿省,位于华北克拉通东缘,由西北部的胶北地体和东南部的苏鲁造山带组成(Zhao *et al.*, 2012; Deng *et al.*, 2022a; Zhang *et al.*,2020).夏甸金矿床位于胶东半岛西北部的NE向招平断裂带内(图1).招平断裂在夏甸金矿区主要沿前寒武变质岩与玲珑花岗岩接触带分布,其上盘为前寒武斜长角闪岩、片麻岩变质岩系,下盘主体为玲珑黑云母二长花岗岩,偶见玢岩、煌斑岩等脉岩(Liu *et al.*, 2021b; Chen *et al.*, 2024b).该断裂在矿区平均产状120°∠40°,走向与倾向呈平缓波动.主断层破碎带构造岩相分带明显,从中心向两侧依次为糜棱岩、强碎裂岩、弱碎裂岩、未变形围岩.此外,断裂下盘发育大量NE/NW向次级断裂与节理,部分次级断裂内充填中基性岩脉(Yang *et al.*, 2016; Liu *et al.*, 2020).夏甸矿床的金矿化具有典型的构造蚀变岩型矿化特征,严格受招平断裂及次级构造控制,赋存于黄铁绢英岩化蚀变带与红化蚀变带中,矿体形态以脉状、似层状、透镜状为主,倾角20°～60°,普遍具分支复合、膨胀夹缩特征(Huang *et al.*,2024; Mao *et al.*,2024b).矿区主要工业矿体分别为VII号、I-II号、道北庄子矿体群,其中VII号矿体是最主要的金矿体,资源量占比超过90%.

夏甸金矿床的成矿动力学背景与胶东地区其他金矿床一致,均形成于晚白垩世华北克拉通大规模减薄的构造背景(Zhao *et al.*, 2018; Goldfarb *et al.*, 2019; Deng *et al.*, 2022b).含金流体主要源自深部,在招平断裂带构造活动的驱动下,含矿热液向浅部运移,通过相分离、水岩反应等机制与随后的矿物自组织作用实现元素分异与富集,最终在不同构造带内形成金矿体(Liu *et al.*, 2018; Deng *et al.*, 2020; Liu *et al.*, 2021a; Huang *et al.*, 2023)(图2).

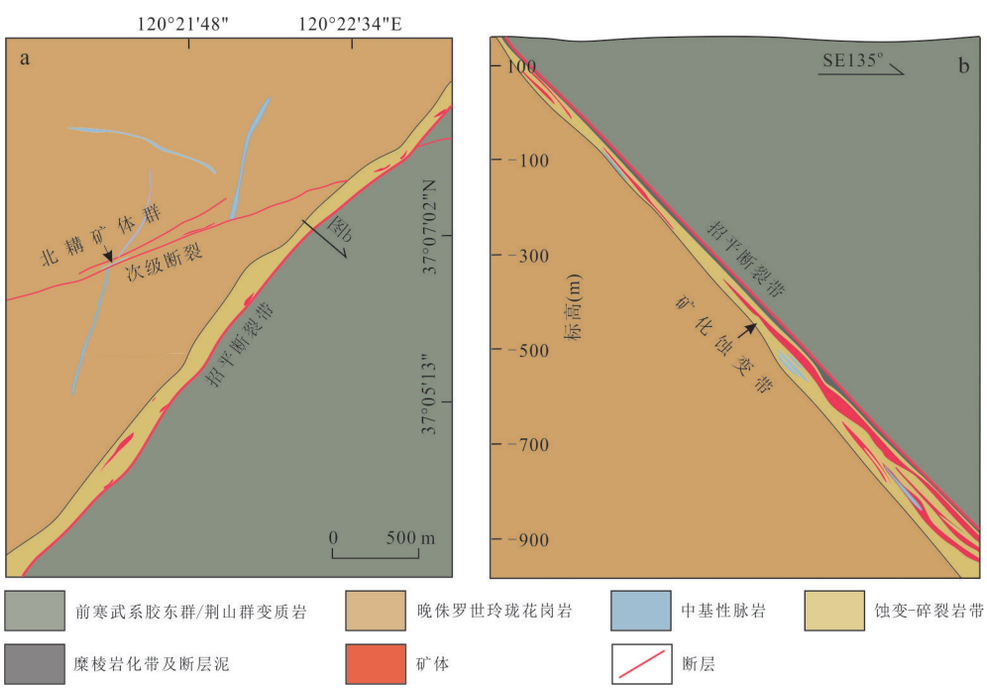

图1　夏甸金矿地质简图(a)与代表性地质剖面(b)

Fig.1　Simplified geology map of the Xiadian gold deposit (a) and its representative cross-section (b)

据Mao *et al.*(2024b)修改

2　方法

本文提出的融合地质先验知识与数据驱动技术的协同建模框架(图 3)主要包括三方面内容:(1)特征提取与建模:基于钻孔编录、勘探剖面及中段平面图等勘查数据,构建研究区高精度三维体元模型,提取流体运移通道相关指标,构建各体元间的空间邻接图结构,实现地质信息的数字化与结构化表达,为后续模型提供输入数据.(2)通道位置概率预测:引入 GCN 处理非欧几里得空间的模型数据,挖掘局部邻域内构造-蚀变-矿化的隐含流体运移信息,在小样本标签(已知流体迹象)约束下,训练分类模型,计算全区每个体元作为流体通道的空间后验概率,生成三维流体通道空间位置概率场.(3)流体运移路径表征:将上述概率场视为状态空间,构建三维马尔科夫链随机模拟模型,结合达西定律与流体动力学机制,定义包含地质趋势项、重力势能项及随机扰动项的转移概率矩阵,追踪成矿流体从深部源区向浅部的"随机游走"轨迹,重建流体运移通道三维结构.

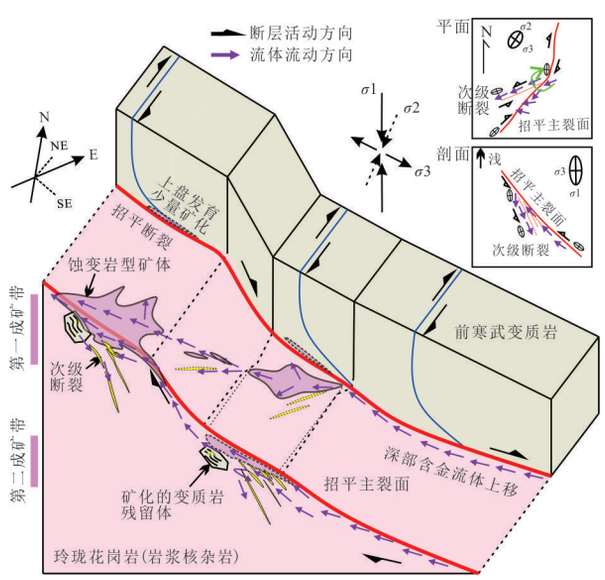

图 2　夏甸金矿成矿概念模型(Liu *et al.*, 2021a)

Fig.2　Conceptual metallogenic model of the Xiadian gold deposit (Liu *et al.*, 2021a)

2.1　GCN

GCN 是一种处理图结构数据的深度学习模型,其核心是将卷积操作从规则的欧几里得数据扩展到不规则的图数据,通过聚合节点自身特征与邻居节点特征,学习图数据的全局和局部结构信息(Kipf and Welling, 2017; Zhou *et al.*, 2020; Wu *et al.*, 2021).GCN 通过在图结构(即 3D 体元邻接关系)上进行多层消息传递,可有效地模拟流体通道位置概率如何受其局部(26 邻域)特征和邻居节点状态的影响(Atwood and Towsley, 2016; Gilmer *et al.*, 2017; Battaglia *et al.*, 2018).这种机制使得 GCN 不仅具有统计分类功能,而且能隐含地表达流体不同时间/空间流动的连续过程(Pfaff *et al.*, 2020; Sanchez-Gonzalez *et al.*, 2020).本文基于成矿空间体元信息,在地质认识驱动下对已知的流体通道位置进行标记,通过 GCN 建立通道标记点与相关地质体特征(断裂、蚀变带、矿体等)的关联关系,进一步计算流体通道的空间位置概率(图 4).

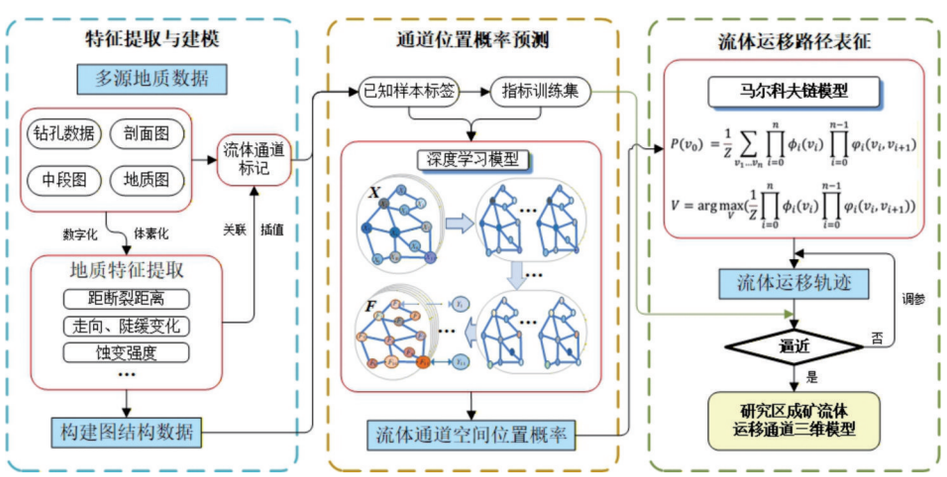

图 3　方法流程图

Fig.3　Workflow of the proposed methodology

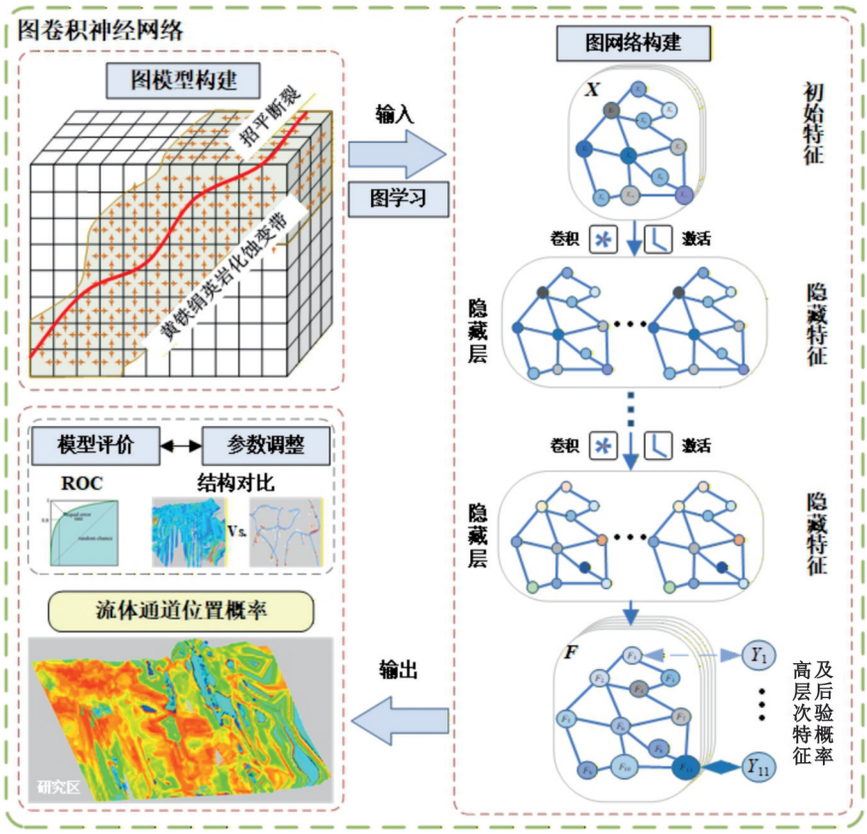

图 4　基于图卷积网络生成流体通道位置概率模型流程

Fig.4　Workflow for generating the fluid pathway probability model based on a graph convolutional network

本文研究中,首先将夏甸矿化-蚀变带内的流体通道模型离散化为规则的体元(Voxel)栅格模型,每个体元都被定义为一个图节点 $v_i \in V$,该过程将连续的地质空间转化为离散的、结构化的数据,为后续的图结构构建奠定基础,体元的数量 N 即为图的节点总数.每个节点承载一个特征向量 X,该向量在本研究中由三维空间坐标和五个与成矿流体流动密切相关的地质特征指标组成(表 1).由于地质调研获取的通道信息是稀疏且受限的,因而用于训练的标签数据(Y)数量有限,本文定义正样本为:结合地质调研区和地质图件中厘定的流体通道识别标志,对通道标记进行离散化,形成流体通道标记三维点集模型.这些点集对应的体元即为正样本.将远离通道标记的已知体元作为负样本,但这些体元仍需位于黄铁绢英岩化蚀变带内.

从成矿系统演化过程角度看,成矿流体运移通道并非单一几何对象,而是由构造连通性、渗透性增强区以及流体-围岩反应过程共同控制形成的优势渗流网络结构(Groves *et al.*, 2018; Hronsky, 2020; Shilunga and Kisters, 2022).本文所选取的指标体系并非经简单统计得到的相关变量集合,而是对流体运移关键过程要素的参数化表达.其中,距控矿断裂距离及断裂几何学参数(走向、陡缓)主要反映构造体系的空间连通性与力学活动性,是流体通道形成与延伸的“结构框架约束”(Cowan, 2020);蚀变带厚度反映成矿流体与构造-围岩的作用程度,是流体运移通量与作用强度的综合响应(Campos *et al.*, 2022);金品位则代表流体在局部物理化学条件变化下的矿质沉淀结果,是通道末端沉淀过程的直接表现(Yardley and Bodnar, 2014).因此,上述指标组合能够共同刻画构造格架下成矿流

表 1　GCN 节点属性(X)和几何输入特征(F=8)

Table 1　GCN node attributes (X) and geometric input features (F=8)

特征类别	特征名称	意义
流体运移驱动	距控矿断裂距离	表达控矿断裂的作用场
	断裂走向	表达控矿断裂的几何学特征
	断裂陡缓	
流体作用产物	蚀变场强(厚度)	表达流体与围岩作用
	金品位值	直接反映矿质的沉淀结果
三维坐标	X、Y、Z	提供空间位置信息

体运移通道的空间分布特征,使模型预测结果具有明确的成矿过程地质内涵与物理意义支撑.

在图结构建模框架下,成矿流体运移通道被视为由优势连通域构成的空间网络结构,而非孤立的点状高值异常.图结构/图神经网络能够在不规则空间采样条件下表达地质体元之间的邻接关系与拓扑结构,从而支持三维地质对象的结构化推断(Hillier *et al.*, 2021).在裂隙介质研究中,连通性指标已被证明可用于快速刻画流动通道特征,并在一定程度上替代高成本的数值流动模拟(Javanmard *et al.*, 2022);同时,裂隙网络的连通性特征与渗透能力之间存在可定量评估的关系(Ye *et al.*, 2021).更重要的是,在区域尺度上优先流动的通道往往主要受连通性控制,而非局部高渗区的点状异常控制(Lin *et al.*, 2023).据此,本文采用图结构下的邻域信息传播与连通性表达,可实现对成矿流体运移通道空间位置概率的整体推断,而非局部相关性的简单拟合.

GCN以图结构数据为输入,通过聚合节点自身及其邻域节点特征,实现对非规则空间结构信息的有效表征(Kipf and Welling, 2017).在三维体元模型中,为刻画成矿流体运移的空间连续性与连通性,本研究将体元视为图节点,并基于体元间的空间邻接关系构建图结构.图模型采用三维体元的26邻域连接方式定义节点间的边关系,该邻域定义能够在三维空间中充分保持斜向及复杂结构方向上的连通性,符合流体在构造-蚀变系统中运移路径的空间特征.邻接矩阵中边的权重依据体元间的空间距离进行设置,以反映近邻体元对流体运移影响更为显著的地质规律特点.

在此基础上,将体元属性特征矩阵与加权邻接矩阵输入图卷积网络进行训练.GCN各层通过邻域特征聚合与非线性映射,逐层提取反映流体通道空间分布特征的高层次信息,其基本形式为:

$$H^{(l)}=\sigma(\tilde{A}H^{(l-1)}W^{(l)}), \tag{1}$$

其中,$\tilde{A}$为经过归一化处理(通常包含自连接)的邻接矩阵,$\sigma(\cdot)$为非线性激活函数,$W^{(l)}$为待学习的参数权重.

在模型结构设计上,网络层数采用浅层结构配置,以避免在样本规模受限条件下引入过拟合风险,同时保证对空间邻域信息的有效聚合能力;隐藏层维度根据节点特征维数及样本规模进行匹配设置,以兼顾特征表达能力与模型训练稳定性.学习率及正则化参数采用小步长策略配置,以增强训练过程的收敛稳定性并降低训练振荡风险.

模型输出层采用全连接层结合Softmax(或LogSoftmax)函数,输出各体元属于流体通道与非通道的概率分布:

$$Z=f_{FC}(H^{(l)}), \tag{2}$$

$$P=Softmax(Z). \tag{3}$$

GCN训练采用半监督学习方式,在利用全体体元特征与图结构进行信息传播的同时,仅对已知流体通道位置的标记体元计算损失函数:

$$L=-\sum_{i\in y_L}\sum_{c=1}^{C}Y_{ic}\ln Z_{ic}(X,A;\Theta). \tag{4}$$

通过最小化交叉熵损失函数并采用Adam优化算法进行参数更新,模型能够在图结构约束下,将有限的标记信息传播至未标记体元,从而实现对研究区内成矿流体运移通道空间位置概率的整体推断.

为验证模型可靠性和准确度,本研究通过ROC曲线等指标评价图卷积网络模型的通道信息学习能力,通过不断调整模型参数,使其对训练样本数据的结果不断逼近真实通道三维点集模型,达到模型性能的最优化.

2.2 马尔科夫链

成矿流体通道空间位置概率数据蕴含了系统的流体通道空间位置信息,反映了流体通道的整体空间展布特征,通道位置高概率体元在三维空间中的有机连接能客观表达流体通道三维结构.构建以体元为基础的马尔科夫链模型(Deng *et al.*, 2024; Huang *et al.*, 2024),将流体运移路径表示为一系列体元的集合,采用马尔科夫链表示该路径联合概率分布:

$$P(V)=\frac{1}{Z}\prod_{i=0}^{n}\phi_i(v_i)\prod_{i=0}^{n-1}\varphi_i(v_i,v_{i+1}), \tag{5}$$

其中,v_i表示流体运移路径上第i个节点所对应的体元,满足$v_i\neq v_{i+1}$且v_i与v_{i+1}存在相互邻接(26-邻接),Z表示归一化常数,$\phi_i(v_i)$为状态函数,表示流体运移路径上第i个节点为体元v_i的势函数,$\varphi_i(v_i,v_{i+1})$为转移函数,表示当流体运移路径上第i个节点为体元v_i时,第$i+1$个节点为体元v_{i+1}的势函数(Murphy, 2012).

路径的概率分布通过状态函数和转移函数联合表达.将状态函数定义为每个体元是流体通道的后验概率,其计算依赖图卷积网络对流体位置的学习结果;转移函数则基于达西定律,结合体元间的位置关系,通过正态分布模型描述流体从一个节点到下一个节点的转移概率,

反映流体流动的方向性和连续性(Rubin,2003;Kang *et al.*,2017;Sherman *et al.*,2021).

状态函数:

$$\phi_i(v_i)=F_{v_i1}=P\left(y_{v_i}=1|X\right), \tag{6}$$

转移函数:

$$\varphi_i(v_i,v_{i+1})=\frac{1}{\sqrt{2\pi}\,\sigma_i}\exp\left(-\frac{\left\|z_{i+1}-\left(z_i+q_it\right)\right\|^2}{2\sigma_i^2}\right), \tag{7}$$

其中,z_i和z_{i+1}体元分别表示v_i和v_{i+1}的空间位置,q_i表示体元v_i处流体的达西流速,σ_i^2为方差.在建模过程中,拟根据流体运移通道推断过程中的相邻体元的相对位置信息,基于动量守恒原则,获得体元v_i处流体的达西流速q_i的方向;基于能量守恒原则,获得体元v_i处流体的达西流速q_i的大小.在此基础上,结合达西定律,进一步修正达西流速q_i.

3　夏甸金矿成矿流体运移通道三维重建

3.1　已知区流体通道相关地质体三维建模

本文收集了夏甸金矿床以往的勘查开采数据,包括坑道和钻孔编录描述、中段平面图、勘探线剖面图等,并对这些数据进行数字化和预处理,采用显式和隐式建模相结合的建模方法,建立了已知区三维矿体模型、控矿断裂模型、蚀变带三维模型(图 5).

3.2　流体通道位置信息挖掘

本文对成矿流体的运移驱动机制因素(招平断裂特征)和成矿流体的作用产物(蚀变带、矿化)开展空间分析并与成矿空间体元进行关联,获得了相关的定量指标集(图 6a~6e).为构建更合理、更具代表性的训练样本数据,笔者结合成矿流体通道认识,根据流体通道体素模型和金矿化程度高低建立不同大小的缓冲区,缓冲区范围内体元作为正样本(n=5 089;图 6f),蚀变带内远离通道标记或地质调查明确否定的体元标记为负样本,并将研究区样品按 9∶1 比例划分为训练集与测试集.

本次训练将GCN模型训练了100个Epoch,模型性能评估是基于对10%独立验证集(67 500个节点)的测试结果.模型在处理类别不平衡问题时,采用了自动计算的类别权重($W_0\approx0.59$,$W_1\approx3.17$),确保对少数类(流体通道)的有效学习.如图 7 所示,模型在100轮训练周期内展现出优秀的稳定性和收敛速度.训练损失持续且平滑地从0.7左右下降至0.323 3,曲线在0到100轮内没有出现振荡或发散现象,多次独立训练结果在通道概率场空间分布格局上保持高度一致性,主通道结构与分支网络形态稳定复现,证明了特征标准化和Batch Normalization(BN)策略可保障GCN在处理大规模数据时的数值稳定性和结构一致性.训练过程中验证集准确率迅速提升,并在100轮训练结束时达到0.848 7,表明模型在较短的训练周期内就实现了对地质特征的高效学习,且具备良好的泛化能力.模型的全局区分能力通过ROC曲线下的面积(Area Under Curve,AUC)进行量化,如图 7c 所示,曲线几乎贴近左上角,AUC值高达0.956 9,证明GCN成功利用了k近邻图所编码的空间拓扑依赖性,使模型具备极强的流体通道与非通道区域的判别能力.

基于上述训练模型,本文对夏甸金矿床的成矿流体运移通道空间位置进行了推断,推断结果如图 8 所示.

3.3　流体通道三维结构重建

GCN模型输出的P_{Channel}是一个静态的、体元级别的通道位置可能性图,该概率图反映了流体通道的整体空间展布,作为输入导入马尔科夫链模型.本研究将流体运移通道的推断问题建模为一个序列决策过程,即马尔科夫链模型下的最大后验概率

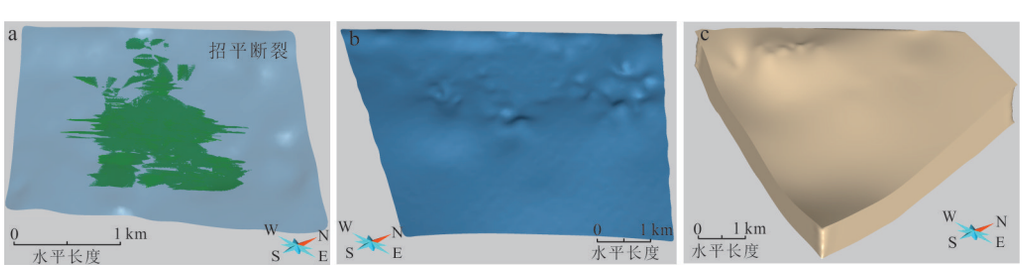

图 5　已知区地质体三维模型

Fig.5　Three-dimensional geological models of the study area

a.金矿体;b.招平断裂;c.绢英岩蚀变带

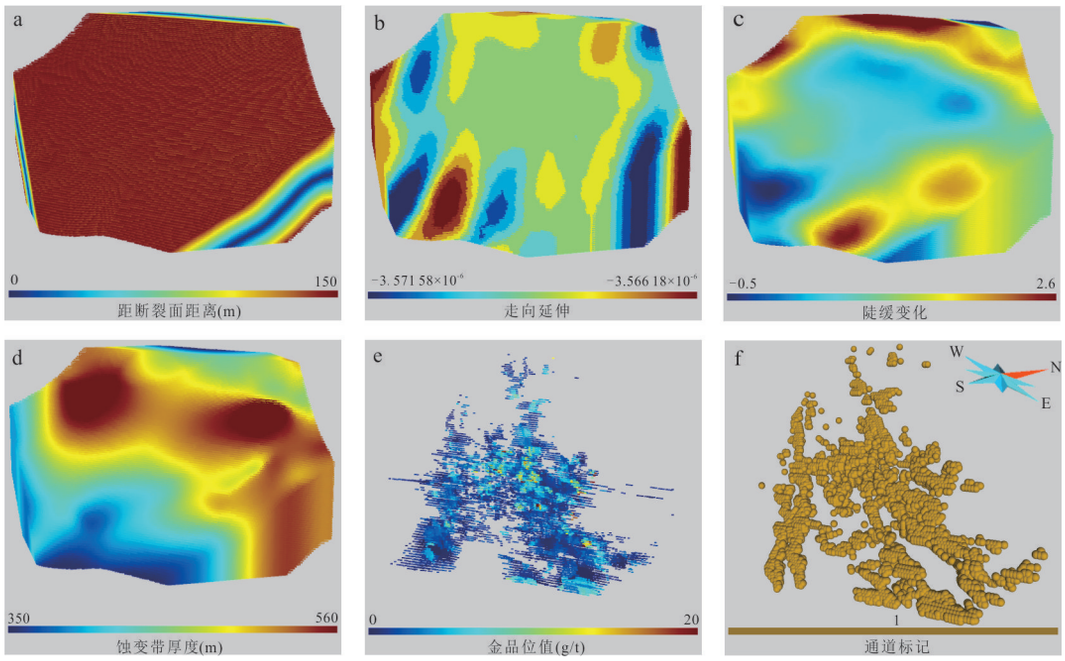

图 6 GCN 建模指标集

Fig.6 Indicator datasets used for GCN modeling

a.距招平断裂距离;b.走向;c.陡缓;d.蚀变带厚度;e.金品位值;f.通道标记

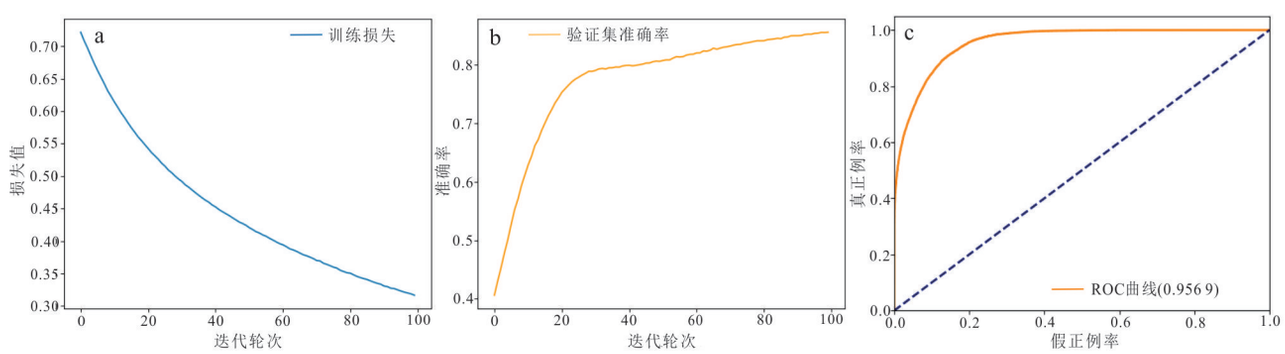

图 7 损失曲线(a)、验证集准确率曲线(b)和 ROC 曲线(c)

Fig.7 Training loss curve (a), validation accuracy curve (b), and ROC curve (c)

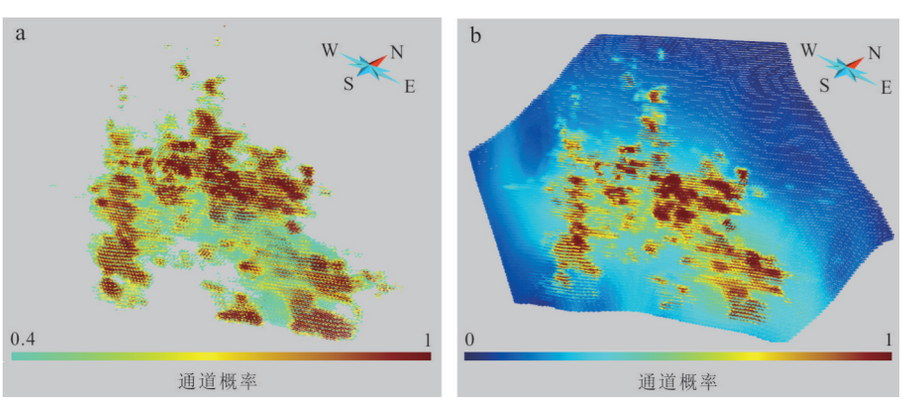

图 8 夏甸金矿床成矿流体通道概率分布(高概率区)(a)和研究区距断裂面 10 m 内通道概率分布(b)

Fig.8 Fluid pathway probability in the Xiadian gold deposit (high) (a), fluid pathway probability within 10 m of the fault surface in the study area (b)

求解和随机采样问题.将三维体元空间视为状态空间,流体在相邻体元之间的运移被视为状态转移(Le Borgne *et al.*, 2008; Kang *et al.*, 2017; Cirpka *et al.*, 2022).通道的重建目标是寻找从深部来源区到浅部目标界面的最优路径(主干通道)和次优路径(次级通道).

基于马尔科夫链的流体运移轨迹推断模型,将流体通道的重建转化为求解最大后验概率问题.通道重建首先对所有体元进行预筛选,只保留通道概率高于0.6分位数且距断层距离小于20 m的体元,以构建KDTree进行高效搜索(Arya *et al.*, 1998; Samet, 2006).路径生长的每一步都是从当前体元v_{i-1}的邻域中选择下一个体元v_i,其选择依据是最大化评分函数$S(v_i \to v_{i-1})$.本方法通过构建一个具有地质过程约束意义的加权评分函数$S(v_i \to v_{i-1})$来近似状态转移概率$P(v_i|v_{i-1}, D_i)$,以指导路径的空间延伸.该评分函数是对成矿流体运移过程中多重控制机制的参数化表达,其本质是将通道连通性控制、构造约束控制、重力势能控制及随机扰动过程,统一纳入到同一状态转移框架中进行综合建模.评分函数在结构上体现"主控因素优先、次级因素调制"的层级约束关系,即以流体通道概率场作为主导控制项,构造连通性作为结构约束项,重力势能与方向趋势作为物理约束项,随机扰动作为自然非线性过程的表达项,从而保证路径延伸过程满足地质合理性兼具自然复杂性与空间曲折性.具体表达式如下,参数设置如表2所示:

$$S = W_{\mathrm{P}} \cdot P_{\mathrm{norm}} - W_{\mathrm{FD}} \cdot FD_{\mathrm{norm}} + W_{\mathrm{DIR}} \cdot \cos(\theta) + W_{\mathrm{DZ}} \cdot \Delta Z + \mathrm{Noise}\ . \tag{8}$$

从成矿过程角度看,各权重项分别对应成矿流体运移过程中的关键控制机制:归一化通道概率项反映流体在优势渗透结构中的优先运移趋势,是流体运移路径形成的主控因子;距断层距离项体现构造变形域内的连通性对流体运移路径选择的空间约束作用,保证路径延伸受主要控矿构造控制;转移方向与上倾地质方向的余弦项反映区域构造应力场与流体运移方向之间的耦合关系,用于维持整体向上运移趋势但允许局部转折;Z轴向上分量项体现重力势能差异对流体运移的物理约束效应;随机扰动项则用于表达非均质介质中流体运移过程的自然随机性与曲折性特征.上述权重组合共同构成"结构约束-物理约束-随机过程"协同控制的状态转移机制,从而使路径模拟结果不仅满足数学意义上的最优性,同时具备明确的地质合理性与解释性.

基于上述方法和参数,重建了夏甸金矿床的流体运移通道网络,结果如图9a、9b所示.重建结果呈现出典型的树状发散结构,两个主要通道作为骨架连接密集的次级通道网络,暗示成矿流体沿主干构造向上,并在构造裂隙或渗透性层位中扩散充填的运移模式.

3.4　成因启示与找矿意义

本文研究显示,夏甸金矿床深部流体通道体系主要由两条近平行、NE向侧伏的流体主通道及其沿断裂面高角度斜交发育的次级流体通道共同构成(图9),整体呈现出"树状"三维结构特征.该结构表明,夏甸金矿床的金矿化并非均匀分布于整个断裂或剪切带中,而是高度集中于少数空间连续性好、运移效率高且稳定性强的优势流体通道之中(图6和图9),反映出流体通道具有明显的导矿-容矿的混合成矿功能.从空间结构上看,深部成矿流体在区域构造应力场控制下,沿特定优势通道向上定向注入,并在通道内部完成局部高效输运与物质富集过程,从而在主通道内部形成高品位矿化集中区.NE向侧伏的流体主通道(图9)可能代表深源流体多期次重复上升的高效注入通道,是控制夏甸金矿床成矿的核心输运体系.因此,可以推断夏甸金矿的成矿过程主要受构造-流体耦合机制控制,即在晚白垩世右旋走滑构造应力场背景下,区域招平断裂带发生拆离运动,形成有利于深部流体定向注

表2　流体运移通道推断模型参数设置

Table 2　Parameter settings used in the fluid pathway inference model

表达式	描述	权重(W)	作用分析
P_{norm}	归一化通道概率	$W_{\mathrm{P}}=4.0$	核心驱动力,路径优先进入高概率体元
FD_{norm}	归一化距断层距离	$W_{\mathrm{FD}}=1.0$	构造约束,惩罚远离断层的路径
$\cos(\theta)$	流体运移方向是否顺应断裂上倾方向	$W_{\mathrm{DIR}}=0.5$	极弱宏观约束,保持向上趋势,但允许局部转折
ΔZ	向上Z轴分量($\geqslant 0$)	$W_{\mathrm{DZ}}=1.5$	重力势能奖励,偏好整体向上运移
Noise	随机扰动项	$W_{\mathrm{Noise}}=0.5$	曲折度控制,引入自然曲折

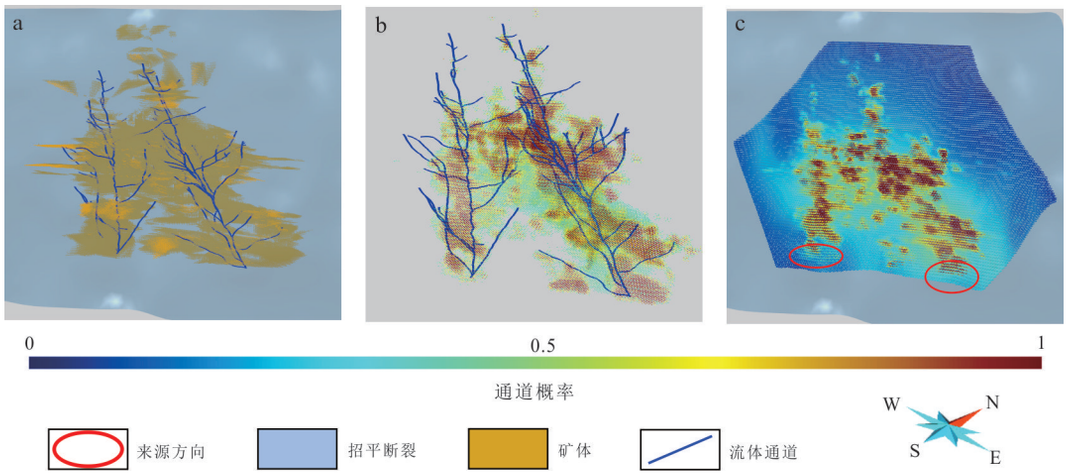

图 9 夏甸金矿床成矿流体运移通道重建

Fig.9 Reconstruction of ore-forming fluid migration in the Xiadian gold deposit

a.成矿流体运移通道与已知矿体;b.成矿流体运移通道与成矿流体通道高概率分布区;c.推断流体来源方向

入的高渗透通道体系(Wang *et al.*, 2019; Deng *et al.*, 2020).在该构造体制下,深部超压流体沿优势的渗透通道发生注入式运移,构建起稳定的成矿流体输运网络结构(图 9).

此外,在夏甸金矿,蚀变带厚度显著增厚部位,流体通道分支程度最高(图 6d;图 9),反映出成矿流体流动过程中由构造几何突变与围岩水岩反应引发的非稳态破裂响应过程(Groves *et al.*, 2018;Cowan, 2020).当流体沿主通道上升并遭遇围岩碎裂程度、渗透性结构或断裂几何条件突变时,局部渗透性降低导致流体暂时滞留与压力积累,进而触发瞬时破裂与侧向扩展,形成次级流体通道网络结构(图 9).在这些部位,构造释压作用与增强的流体-岩石相互作用共同促进蚀变作用显著加强(Mao *et al.*, 2024b),并加速金从成矿流体中的析出与富集,形成厚大矿化蚀变带.

基于流体通道三维结构模型,本文进一步圈定了夏甸金矿床深部两个成矿有利区(图 9c 红圈所示),其主要分布于深部流体主通道在侧伏方向上的深部延伸部位,显示预测靶区并非孤立异常,且处于深源流体持续注入与物质汇聚的优势结构位置,因此具备较高的成矿潜力与找矿价值.夏甸金矿最新的生产勘探工作显示,在-1020 中段的北巷 566-574 线和南巷 520-529 线(分别对应两个成矿有利区)均揭露构造蚀变岩型金矿体.因此,本文提出的流体通道重建方法在实践应用中,具有可靠的成因启示与找矿勘查参考价值.

4 结论与展望

本文提出了基于图卷积网络与马尔科夫链协同的流体通道重建方法,该方法通过图拓扑结构有效聚合了局部邻域特征,准确预测了流体通道的空间概率分布,进而基于马尔科夫链模型模拟出具有地质合理性的流体连续空间运移轨迹,实现成矿流体运移通道的三维重建.基于该方法,本文建立了夏甸金矿流体运移通道三维结构模型,揭示了夏甸金矿床主通道与次级通道组成的“树状”流体运移网络结构,主干通道具有高通量、强连续性特征,主要承担成矿流体的输运功能,而次级通道网络则对应流速减缓、流体-围岩反应强烈的扩容空间.基于夏甸金矿的流体通道三维结构特征,笔者圈定了夏甸金矿深部找矿有利区并发现了经济矿体.

本文提出的成矿流体运移通道三维重建方法优势在于能够在缺乏完整物理参数条件下,从已有地质数据和认识出发,识别潜在的主要流体通道结构.但该方法本质上属于知识-数据协同驱动的结构推断方法,尚未引入流体力学、热力学及应力-应变演化等多物理场过程的连续性约束,在一定程度上限制了结果的精确度.未来工作中,可将本文识别的三维流体通道结构作为多物理场数值模拟的重要先验约束条件,引入流体动力学、热-力-化学耦合过程,优化流体通道结构,并探讨其形成与演化机制,从而实现数据驱动方法与物理机理模拟的有机融合.

References

An, W. T., Chen, J. P., Zhu, P. F., 2021. A Two-Way Forecasting Method Based on Numerical Simulation of Mineralization Process for the Prediction of Concealed Ore Deposits. *Earth Science Frontiers*, 28(3): 97－111 (in Chinese with English abstract).

Arya, S., Mount, D. M., Netanyahu, N. S., et al., 1998. An Optimal Algorithm for Approximate Nearest Neighbor Searching Fixed Dimensions. *Journal of the ACM*, 45(6): 891－923. https://doi.org/10.1145/293347.293348

Atwood, J., Towsley, D., 2016. Diffusion-Convolutional Neural Networks. 29th Conference on Neural Information Processing Systems (NIPS 2016), Barcelona.

Battaglia, P. W., Hamrick, J. B., Bapst, V., et al., 2018. Relational Inductive Biases, Deep Learning, and Graph Networks. *arXiv*, 1806.01261. https://arxiv.org/abs/1806.01261

Campos, L. M., Toledo, C. L. B., Silva, A. M., et al., 2022. The Hydrothermal Footprint of the Crixás Deposit: New Vectors for Orogenic Gold Exploration in Central Brazil. *Ore Geology Reviews*, 146: 104925. https://doi.org/10.1016/j.oregeorev.2022.104925

Chai, P., Hou, Z. Q., Zhang, Z. Y., 2017. Geology, Fluid Inclusion and Stable Isotope Constraints on the Fluid Evolution and Resource Potential of the Xiadian Gold Deposit, Jiaodong Peninsula. *Resource Geology*, 67(3): 341－359. https://doi.org/10.1111/rge.12134

Chen, G. H., Liu, Z. K., Chen, G. D., et al., 2024a. Deep Gold Prospectivity Modeling in the Jiaojia Gold Belt, Jiaodong Peninsula, Eastern China Using Machine Learning of Geometric and Geodynamic Variables. *Frontiers in Earth Science*, 12: 1308426. https://doi.org/10.3389/feart.2024.1308426

Chen, J., Mao, X. C., Deng, H., et al., 2020. Three-Dimensional Modelling of Alteration Zones Based on Geochemical Exploration Data: An Interpretable Machine-Learning Approach *via* Generalized Additive Models. *Applied Geochemistry*, 123: 104781. https://doi.org/10.1016/j.apgeochem.2020.104781

Chen, Y. D., Liu, Z. K., Wang, R. C., et al., 2024b. New Insights into the Metallogenic Genesis of the Xiadian Au Deposit, Jiaodong Peninsula, Eastern China: Constraints from Integrated Rutile In-Situ Geochemical Analysis and Machine Learning Discrimination. *Ore Geology Reviews*, 171: 106184. https://doi.org/10.1016/j.oregeorev.2024.106184

Cheng, Q. M., 2025. A New Paradigm for Mineral Resource Prediction Based on Human Intelligence-Artificial Intelligence Integration. *Earth Science Frontiers*, 32(4): 1－19 (in Chinese with English abstract).

Cirpka, O. A., Stettler, M. M., Dentz, M., 2022. Spatial Markov Model for the Prediction of Travel-Time-Based Solute Dispersion in Three-Dimensional Heterogeneous Media. *Water Resources Research*, 58(6): e2022WR032215. https://doi.org/10.1029/2022WR032215

Cowan, E. J., 2020. Deposit-Scale Structural Architecture of the Sigma-Lamaque Gold Deposit, Canada—Insights from a Newly Proposed 3D Method for Assessing Structural Controls from Drill Hole Data. *Mineralium Deposita*, 55(2): 217－240. https://doi.org/10.1007/s00126-019-00949-6

Deng, H., Huang, J. X., Liu, Z. K., et al., 2024. Hidden Markov Model for Spatial Analysis of Three-Dimensional Mineralization Distribution: Insights into Magma Flow and Mineral Exploration Targets in the Jinchuan Ni-Cu-(PGE) Sulfide Deposit, China. *Applied Geochemistry*, 162: 105911. https://doi.org/10.1016/j.apgeochem.2024.105911

Deng, H., Zheng, Y., Chen, J., et al., 2022a. Learning 3D Mineral Prospectivity from 3D Geological Models Using Convolutional Neural Networks: Application to a Structure-Controlled Hydrothermal Gold Deposit. *Computers & Geosciences*, 161: 105074. https://doi.org/10.1016/j.cageo.2022.105074

Deng, J., Sun, Z. S., Wang, Q. F., et al., 2003. Crust-Mantle Structures and Gold Enrichment Mechanism of Mantle Fluid System. *Chinese Journal of Geochemistry*, 22(3): 263－270. https://doi.org/10.1007/BF02842870

Deng, J., Wang, Q. F., Liu, X. F., et al., 2022b. The Formation of the Jiaodong Gold Province. *Acta Geologica Sinica* (*English Edition*), 96(6): 1801－1820. https://doi.org/10.1111/1755-6724.15026

Deng, J., Wang, Q. F., Yang, L. Q., et al., 2005. An Analysis of the Interior Structure of the Gold Hydrothermal Metallogenic System of the Northwestern Jiaodong Peninsula, Shandong Province. *Earth Science*, 30(1): 102－108 (in Chinese with English abstract).

Deng, J., Yang, L. Q., Groves, D. I., et al., 2020. An Integrated Mineral System Model for the Gold Deposits of the Giant Jiaodong Province, Eastern China. *Earth-Science Reviews*, 208: 103274. https://doi.org/10.1016/j.earscirev.2020.103274

Gilmer, J., Schoenholz, S. S., Riley, P. F., et al., 2017. Neural Message Passing for Quantum Chemistry. 34th International Conference on Machine Learning, Sydney.

Goldfarb, R., Qiu, K., Deng, J., et al., 2019. Orogenic Gold Deposits of China. In: Chang, Z. S., Goldfarb, R. J., eds., Mineral Deposits of China, Society of Economic Geologists, Littleton. https://doi. org/10.5382/SP.22.08

Groves, D. I., Santosh, M., Goldfarb, R. J., et al., 2018. Structural Geometry of Orogenic Gold Deposits: Implications for Exploration of World-Class and Giant Deposits. *Geoscience Frontiers*, 9(4): 1163－1177. https://doi.org/10.1016/j.gsf.2018.01.006

Guo, J. T., Liu, Y. H., Han, Y. F., et al., 2019. Implicit 3D Geological Modeling Method for Borehole Data Based on Machine Learning. *Journal of Northeastern University* (*Natural Science*), 40(9): 1337－1342 (in Chinese with English abstract).

Guo, T., Deng, J., Lü, G. X., et al., 2008. The Channel Way, Style and Driving Mechanism of Ore Fluid Migration in the Jiaojia Gold Deposit. *Acta Geoscientica Sinica*, 29(1): 81－88 (in Chinese with English abstract).

Han, R. S., Liu, F., Zhang, Y., 2025. Discussion on Ore-Controlling Roles of Structural System in Hydrothermal Metallogenic System. *Earth Science Frontiers*, 32(2): 371－389 (in Chinese with English abstract).

Henry, A. D., McInnes, P., Tosdal, R. M., 2014. Structural Evolution of Auriferous Veins at the Endeavour 42 Gold Deposit, Cowal Mining District, NSW, Australia. *Economic Geology*, 109(4): 1051－1077. https://doi.org/10.2113/econgeo.109.4.1051

Hickey, K. A., Ahmed, A. D., Barker, S. L. L., et al., 2014. Fault-Controlled Lateral Fluid Flow underneath and into a Carlin-Type Gold Deposit: Isotopic and Geochemical Footprints. *Economic Geology*, 109(5): 1431－1460. https://doi.org/10.2113/econgeo.109.5.1431

Hillier, M., Wellmann, F., Brodaric, B., et al., 2021. Three-Dimensional Structural Geological Modeling Using Graph Neural Networks. *Mathematical Geosciences*, 53(8): 1725－1749. https://doi.org/10.1007/s11004-021-09945-x

Hood, S. B., Cracknell, M. J., Gazley, M. F., et al., 2019. Element Mobility and Spatial Zonation Associated with the Archean Hamlet Orogenic Au Deposit, Western Australia: Implications for Fluid Pathways in Shear Zones. *Chemical Geology*, 514: 10－26. https://doi.org/10.1016/j.chemgeo.2019.03.022

Hou, W. S., Wu, X. C., Liu, X. G., 2007. 3D Sealed Geological Block Modeling with Wire Frame Component. *Journal of Jilin University* (*Earth Science Edition*), 37(5): 1047－1051 (in Chinese with English abstract).

Hronsky, J. M. A., 2020. Deposit-Scale Structural Controls on Orogenic Gold Deposits: An Integrated, Physical Process-Based Hypothesis and Practical Targeting Implications. *Mineralium Deposita*, 55(2): 197－216. https://doi.org/10.1007/s00126-019-00918-z

Huang, J. X., Deng, H., Mao, X. C., et al., 2023. 3D Modeling of Detachment Faults in the Jiaodong Gold Province, Eastern China: A Bayesian Inference Perspective and Its Exploration Implications. *Ore Geology Reviews*, 154: 105307. https://doi.org/10.1016/j.oregeorev.2023.105307

Huang, J. X., Deng, H., Mao, X. C., et al., 2024. A Global-Local Collaborative Approach to Quantifying Spatial Non-Stationarity in Three-Dimensional Mineral Prospectivity Modeling. *Ore Geology Reviews*, 168: 106069. https://doi.org/10.1016/j.oregeorev.2024.106069

Javanmard, H., Saar, M. O., Vogler, D., 2022. On the Applicability of Connectivity Metrics to Rough Fractures under Normal Stress. *Advances in Water Resources*, 161: 104122. https://doi.org/10.1016/j.advwatres.2022.104122

Kang, P. K., Dentz, M., Le Borgne, T., et al., 2017. Anomalous Transport in Disordered Fracture Networks: Spatial Markov Model for Dispersion with Variable Injection Modes. *Advances in Water Resources*, 106: 80－94. https://doi.org/10.1016/j.advwatres.2017.03.024

Kipf, T. N., Welling, M., 2017. Semi-Supervised Classification with Graph Convolutional Networks. *arXiv*, 1609.02907. https://arxiv.org/abs/1609.02907

Koegelenberg, C., Kisters, A. F. M., Harris, C., 2016. Structural Controls of Fluid Flow and Gold Mineralization in the Easternmost Parts of the Karagwe-Ankole Belt of North-Western Tanzania. *Ore Geology Reviews*, 77: 332－349. https://doi.org/10.1016/j.oregeorev.2016.03.010

Launay, G., Sizaret, S., Guillou-Frottier, L., et al., 2018. Deciphering Fluid Flow at the Magmatic-Hydrothermal Transition: A Case Study from the World-Class Panasqueira W-Sn-(Cu) Ore Deposit (Portugal). *Earth and Planetary Science Letters*, 499: 1－12. https://doi.org/10.1016/j.epsl.2018.07.012

Le Borgne, T., Dentz, M., Carrera, J., 2008. Spatial Markov Processes for Modeling Lagrangian Particle Dynamics in Heterogeneous Porous Media. *Physical Review E*, 78(2): 026308. https://doi.org/10.1103/physreve.78.026308

Li, Z. H., Chi, G. X., Bethune, K. M., et al., 2017. Struc-

tural Controls on Fluid Flow during Compressional Reactivation of Basement Faults: Insights from Numerical Modeling for the Formation of Unconformity-Related Uranium Deposits in the Athabasca Basin, Canada. *Economic Geology*, 112(2): 451−466. https://doi.org/10.2113/econgeo.112.2.451

Lin, J. J., Ma, R., Sun, Z. Y., et al., 2023. Assessing the Connectivity of a Regional Fractured Aquifer Based on a Hydraulic Conductivity Field Reversed by Multi-Well Pumping Tests and Numerical Groundwater Flow Modeling. *Journal of Earth Science*, 34(6): 1926−1939. https://doi.org/10.1007/s12583-022-1674-5

Liu, J. C., Wang, J. Y., Liu, Y., et al., 2018. Ore Genesis of the Xiadian Gold Deposit, Jiaodong Peninsula, East China: Information from Fluid Inclusions and Mineralization. *Geological Journal*, 53(S1): 77−95. https://doi.org/10.1002/gj.3042

Liu, X. F., Deng, J., Liang, Y. Y., et al., 2020. Geochemical, Mineralogical and Chronological Studies of Mafic-Intermediate Dykes in the Jiaodong Peninsula: Implications for Late Mesozoic Mantle Source Metasomatism and Lithospheric Thinning of the Eastern North China Craton. *International Geology Review*, 62(18): 2239−2260. https://doi.org/10.1080/00206814.2019.1692253

Liu, Z. K., Chen, J., Mao, X. C., et al., 2021a. Spatial Association between Orogenic Gold Mineralization and Structures Revealed by 3D Prospectivity Modeling: A Case Study of the Xiadian Gold Deposit, Jiaodong Peninsula, China. *Natural Resources Research*, 30(6): 3987−4007. https://doi.org/10.1007/s11053-021-09956-9

Liu, Z. K., Hollings, P., Mao, X. C., et al., 2021b. Metal Remobilization from Country Rocks into the Jiaodong-Type Orogenic Gold Systems, Eastern China: New Constraints from Scheelite and Galena Isotope Results at the Xiadian and Majiayao Gold Deposits. *Ore Geology Reviews*, 134: 104126. https://doi.org/10.1016/j.oregeorev.2021.104126

Mao, X. C., Chen, Y. D., Liu, Z. K., et al., 2024b. Hydrothermal Alteration and Its Geochemistry of the Xiadian Gold Deposit, Jiaodong Peninsula, China: Implications for Fluid-Rock Interaction Processes and Mineral Exploration. *Ore Geology Reviews*, 170: 106134. https://doi.org/10.1016/j.oregeorev.2024.106134

Mao, X. C., Deng, H., Chen, J., et al., 2024. Theory and Methods for Three-Dimensional Intelligent Prospectivity Mapping of Deep Resources in Metal Mines. *Mineral Exploration*, 15(8): 1365−1378 (in Chinese with English abstract).

Mao, X. C., Duan, X. M., Deng, H., et al., 2026. Intelligent 3D Prediction of Deep Mineral Resources: Theory, Methods, and Challenges. *Earth Science*, 51(3): 793−815 (in Chinese with English abstract).

Mao, X. C., Zhong, H. T., Liu, Z. K., et al., 2024a. 3D Numerical Modeling for Investigating Structural Controls on Orogenic Gold Mineralization, Sanshandao Gold Belt, Eastern China. *Natural Resources Research*, 33(4): 1413−1437. https://doi.org/10.1007/s11053-024-10353-1

Murphy, K. P., 2012. Machine Learning: A Probabilistic Perspective. MIT Press, Cambridge.

Pfaff, T., Fortunato, M., Sanchez-Gonzalez, A., Battaglia, P., 2020. Learning Mesh-Based Simulation with Graph Networks. International Conference on Learning Representations 2020, Online.

Rubin, Y., 2003. Applied Stochastic Hydrogeology. Oxford University Press, Oxford.

Samet, H., 2006. Foundations of Multidimensional and Metric Data Structures. Morgan Kaufmann, San Francisco.

Sanchez-Gonzalez, A., Godwin, J., Pfaff, T., et al., 2020. Learning to Simulate Complex Physics with Graph Networks. *arXiv*, 2002.09405. https://arxiv.org/abs/2002.09405

Sherman, T., Engdahl, N. B., Porta, G., et al., 2021. A Review of Spatial Markov Models for Predicting Pre-Asymptotic and Anomalous Transport in Porous and Fractured Media. *Journal of Contaminant Hydrology*, 236: 103734. https://doi.org/10.1016/j.jconhyd.2020.103734

Shilunga, J., Kisters, A., 2022. Lithological and Structural Controls of Disseminated-Type Orogenic Gold Mineralization in High-Grade Metamorphic Turbidites from the Central Zone of the Damara Belt, Namibia. *Ore Geology Reviews*, 151: 105205. https://doi.org/10.1016/j.oregeorev.2022.105205

Sibson, R. H., Robert, F., Poulsen, K. H., 1988. High-Angle Reverse Faults, Fluid-Pressure Cycling, and Mesothermal Gold-Quartz Deposits. *Geology*, 16(6): 551. https://doi.org/10.1130/0091-7613(1988)0160551:harfp>2.3.co;2

Torremans, K., Kyne, R., Doyle, R., et al., 2018. Controls on Metal Distributions at the Lisheen and Silvermines Deposits: Insights into Fluid Flow Pathways in Irish-Type Zn-Pb Deposits. *Economic Geology*, 113(7): 1455−1477. https://doi.org/10.5382/econgeo.2018.4598

Wang, S. R., Yang, L. Q., Wang, J. G., et al., 2019. Geostatistical Determination of Ore Shoot Plunge and Structural Control of the Sizhuang World-Class Epizonal Orogenic Gold Deposit, Jiaodong Peninsula, China. *Minerals*, 9(4): 214. https://doi.org/10.3390/min9040214

Wang, Z. Y., Wang, D., Qiu, K. F., et al., 2025. Applications and Perspectives of Machine Learning in Geochemical Big Data Mining of Minerals and Rocks. *Journal of Chengdu University of Technology* (*Science & Technology Edition*), 52(5): 844－858 (in Chinese with English abstract).

Wu, Z. H., Pan, S. R., Chen, F. W., et al., 2021. A Comprehensive Survey on Graph Neural Networks. *IEEE Transactions on Neural Networks and Learning Systems*, 32(1): 4－24. https://doi. org/10.1109/TNNLS.2020.2978386

Xiang, J., Xiao, K. Y., Carranza, E. J. M., et al., 2020. 3D Mineral Prospectivity Mapping with Random Forests: A Case Study of Tongling, Anhui, China. *Natural Resources Research*, 29(1): 395－414. https://doi. org/10.1007/s11053-019-09578-2

Xiao, F., Chen, X. Y., Cheng, Q. M., 2024. Combining Numerical Modeling and Machine Learning to Predict Mineral Prospectivity: A Case Study from the Fankou Pb-Zn Deposit, Southern China. *Applied Geochemistry*, 160: 105857. https://doi. org/10.1016/j. apgeochem.2023.105857

Xiong, Y. H., Zuo, R. G., 2020. Recognizing Multivariate Geochemical Anomalies for Mineral Exploration by Combining Deep Learning and One-Class Support Vector Machine. *Computers & Geosciences*, 140: 104484. https://doi.org/10.1016/j.cageo.2020.104484

Yang, K. F., Fan, H. R., Santosh, M., et al., 2012. Reactivation of the Archean Lower Crust: Implications for Zircon Geochronology, Elemental and Sr-Nd-Hf Isotopic Geochemistry of Late Mesozoic Granitoids from Northwestern Jiaodong Terrane, the North China Craton. *Lithos*, 146: 112－127. https://doi. org/10.1016/j. lithos.2012.04.035

Yang, L. Q., Deng, J., Wang, Z. L., et al., 2016. Relationships between Gold and Pyrite at the Xincheng Gold Deposit, Jiaodong Peninsula, China: Implications for Gold Source and Deposition in a Brittle Epizonal Environment. *Economic Geology*, 111(1): 105－126. https://doi.org/10.2113/econgeo.111.1.105

Yang, L. Q., Yang, W., Zhang, L., et al., 2024. Developing Structural Control Models for Hydrothermal Metallogenic Systems: Theoretical and Methodological Principles and Applications. *Earth Science Frontiers*, 31(1): 239－266 (in Chinese with English abstract).

Yang, L., Zhao, R., Wang, Q. F., et al., 2018. Fault Geometry and Fluid-Rock Reaction: Combined Controls on Mineralization in the Xinli Gold Deposit, Jiaodong Peninsula, China. *Journal of Structural Geology*, 111: 14－26. https://doi.org/10.1016/j.jsg.2018.03.009

Yardley, B. W. D., Bodnar, R. J., 2014. Fluids in the Continental Crust. *Geochemical Perspectives*, 3(1): 1－127. https://doi.org/10.7185/geochempersp.3.1

Ye, Z. Y., Fan, X. C., Zhang, J., et al., 2021. Evaluation of Connectivity Characteristics on the Permeability of Two-Dimensional Fracture Networks Using Geological Entropy. *Water Resources Research*, 57(10): e2020WR029289. https://doi.org/10.1029/2020WR029289

Zhai, Y. S., 1999. On the Metallogenic System. *Earth Science Frontiers*, 6(1): 13－27 (in Chinese with English abstract).

Zhang, L., Groves, D. I., Yang, L. Q., et al., 2020. Relative Roles of Formation and Preservation on Gold Endowment along the Sanshandao Gold Belt in the Jiaodong Gold Province, China: Importance for Province-toDistrict-Scale Gold Exploration. *Mineralium Deposita*, 55(2): 325－344. https://doi. org/10.1007/s00126-019-00908-1

Zhao, R., Wang, Q. F., Liu, X. F., et al., 2018. Uplift History of the Jiaodong Peninsula, Eastern North China Craton: Implications for Lithosphere Thinning and Gold Mineralization. *Geological Magazine*, 155(4): 979－991. https://doi.org/10.1017/s0016756816001254

Zhao, Z., Zhao, Z. X., Xu, J. R., 2012. Velocity Structure Heterogeneity and Tectonic Motion in and around the Tan-Lu Fault of China. *Journal of Asian Earth Sciences*, 57: 6－14. https://doi.org/10.1016/j.jseaes.2012.05.019

Zhou, J., Cui, G. Q., Hu, S. D., et al., 2020. Graph Neural Networks: A Review of Methods and Applications. *AI Open*, 1: 57－81. https://doi.org/10.1016/j.aiopen.2021.01.001

Zhou, Y. Z., Xiao, F., 2024. Overview: A Glimpse of the Latest Advances in Artificial Intelligence and Big Data Geoscience Research. *Earth Science Frontiers*, 31(4): 1－6 (in Chinese with English abstract).

Zuo, R. G., 2020. Geodata Science-Based Mineral Prospectivity Mapping: A Review. *Natural Resources Research*, 29(6): 3415－3424. https://doi. org/10.1007/s11053-020-09700-9

Zuo, R. G., 2021. Data Science-Based Theory and Method

of Quantitative Prediction of Mineral Resources. *Earth Science Frontiers*, 28(3): 49－55 (in Chinese with English abstract).

Zuo, R. G., Peng, Y., Li, T., et al., 2021. Challenges of Geological Prospecting Big Data Mining and Integration Using Deep Learning Algorithms. *Earth Science*, 46(1): 350－358 (in Chinese with English abstract).

Zuo, R. G., Xu, Y., 2023. Graph Deep Learning Model for Mapping Mineral Prospectivity. *Mathematical Geosciences*, 55(1): 1－21. https://doi. org/10.1007/s11004 - 022-10015-z

Zuo, R. G., Zhang, Z. J., Yang, F. F., et al., 2026. Big Data and Artificial Intelligence-Driven Mineral Prospectivity Mapping. *Earth Science*, 51(3): 779－792 (in Chinese with English abstract).

中文参考文献

安文通, 陈建平, 朱鹏飞, 2021. 基于成矿过程数值模拟的隐伏矿双向预测研究. 地学前缘, 28(3): 97－111.

成秋明, 2025. 面向人类智能与人工智能融合的矿产资源预测新范式. 地学前缘, 32(4): 1－19.

邓军, 王庆飞, 杨立强, 等, 2005. 胶东西北部金热液成矿系统内部结构解析. 地球科学, 30(1): 102－108.

郭甲腾, 刘寅贺, 韩英夫, 等, 2019. 基于机器学习的钻孔数据隐式三维地质建模方法. 东北大学学报(自然科学版), 40(9): 1337－1342.

郭涛, 邓军, 吕古贤, 等, 2008. 焦家金矿床成矿流体运移的通道、方式及驱动机制. 地球学报, 29(1): 81－88.

韩润生, 刘飞, 张艳, 2025. 论热液成矿系统中构造体系控矿作用. 地学前缘, 32(2): 371－389.

侯卫生, 吴信才, 刘修国, 2007. 基于线框单元体的三维闭合地质块体构建方法. 吉林大学学报(地球科学版), 37(5): 1047－1051.

毛先成, 邓浩, 陈进, 等, 2024. 金属矿山深部资源三维智能预测理论与方法. 矿产勘查, 15(8): 1365－1378.

毛先成, 段新明, 邓浩, 等, 2026. 深部矿产三维智能预测理论、方法与挑战. 地球科学, 51(3): 793－815.

王智宇, 王达, 邱昆峰, 等, 2025. 机器学习在矿物岩石地球化学大数据挖掘中的应用与展望. 成都理工大学学报(自然科学版), 52(5): 844－858.

杨立强, 杨伟, 张良, 等, 2024. 热液成矿系统构造控矿理论. 地学前缘, 31(1): 239－266.

翟裕生, 1999. 论成矿系统. 地学前缘, 6(1): 13－27.

周永章, 肖凡, 2024. 管窥人工智能与大数据地球科学研究新进展. 地学前缘, 31(4): 1－6.

左仁广, 2021. 基于数据科学的矿产资源定量预测的理论与方法探索. 地学前缘, 28(3): 49－55.

左仁广, 彭勇, 李童, 等, 2021. 基于深度学习的地质找矿大数据挖掘与集成的挑战. 地球科学, 46(1): 350－358.

左仁广, 张振杰, 杨帆帆, 等, 2026. 大数据人工智能驱动的矿产预测. 地球科学, 51(3): 779－792.